ACS APPLIED POLYMER MATERIALS

pubs.acs.org/acsapm Article

Bio-Inspired Platelet-Reinforced Polymers with Enhanced Stiffness and Damping Behavior

Wilhelm Woigk, Kunal Masania,* Fabian Stork, Alex Heusi, Erik Poloni, and André R. Studart*

Cite This: ACS Appl. Polym. Mater. 2020, 2, 3557−3565 Read Online

ACCESS | Metrics & More | Article Recommendations | SI Supporting Information

ABSTRACT: Structural materials combining high stiffness and damping capabilities are in high demand for passive damping applications in vibration control, precision manufacturing, and resilient buildings. However, the development of enhanced passive damping materials with high stiffness at low weight has been hindered by the mutually excluding nature of these mechanical properties. Motivated by the mechanical performance of biological materials such as bone and nacre, we exploit a simple casting and magnetically assisted manufacturing process to fabricate platelet-reinforced polymers with a stiff and damping staggered architecture. Dynamic mechanical analysis of our staggered architectures reveals an increase in the stiffness of the composites by a factor up to 4.5 while maintaining the strong damping response of the host polymer. Using an established micromechanical model, we can predict the damping figure of merit of such composites and provide guidelines for the creation of stiff and damping bio-inspired structures while considering boundary conditions of the manufacturing process. By reaching mechanical performance superior or comparable to bone and nacre, our bio-inspired strategy proves to be a promising pathway for the further development of low-power passive damping materials.

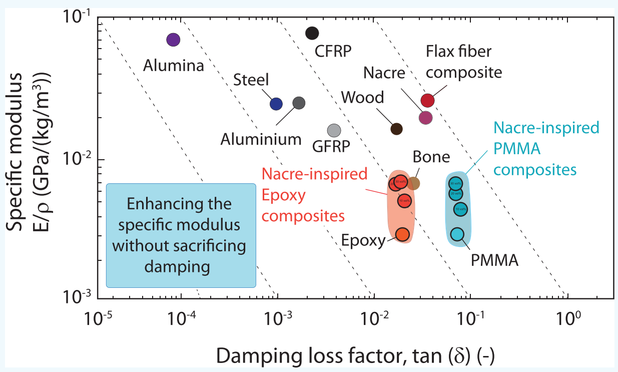

KEYWORDS: *platelets, passive damping, staggered, alumina, polymers*

INTRODUCTION

Damping materials are useful for the reduction of mechanical vibration in applications ranging broadly from semiconductor manufacturing,[1] to noise control and attenuation,[2] to the construction of earthquake-resilient buildings.[3] While active damping strategies have been proposed and effectively exploited, passive damping through structural materials is an attractive approach because it does not require input energy and is thus readily deployable in any structural application. However, enhanced passive damping often comes at the cost of lower mechanical stiffness and strength. This trade-off between damping and stiffness is readily manifested in many examples across different single materials classes and explains why ringing bells are stiff and damping egg cartons are soft.

Composites offer an attractive pathway to reconcile these antagonistic properties by combining stiff and energy dissipating elements in the same material. Viscoelastic polymers reinforced with microscale fibers or nanofillers have been extensively investigated as a means to create composites for enhanced stiffness and damping performance. Despite the improved damping properties achieved in many of these systems, the trade-off between stiffness and damping properties is often observed. Typically, the reinforcement of polymers with continuous or discontinuous microfibers (diameter ∼ 10 μm) leads to high stiffness but does not provide the high interfacial area needed for enhanced energy dissipation.[4−7] By contrast, the use of nanofillers as reinforcing elements improves the damping response of viscoelastic polymers but is not sufficient to achieve high stiffness due to the low volume fraction of solids, typically below 5%.[8−10] To address these limitations, composites with reinforcement architectures that combine high concentrations of stiff elements and a high stiff−soft interfacial area remain in high demand. Inorganic platelets with submicrometer thickness are known to effectively reinforce polymers,[11−15] but the resulting composites have not yet been investigated in terms of damping properties. In more recent work, a composite architecture, comprising a stiff polymer matrix loaded with inorganic spherical fillers coated by a thin layer of a dissipative polymer, has shown to exhibit an unusual combination of high stiffness and energy dissipation.[16] This highlights the importance of the composite architecture on improving the damping performance of structural materials.

Received: May 28, 2020
Accepted: July 15, 2020
Published: July 15, 2020

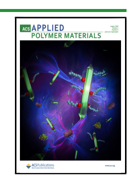

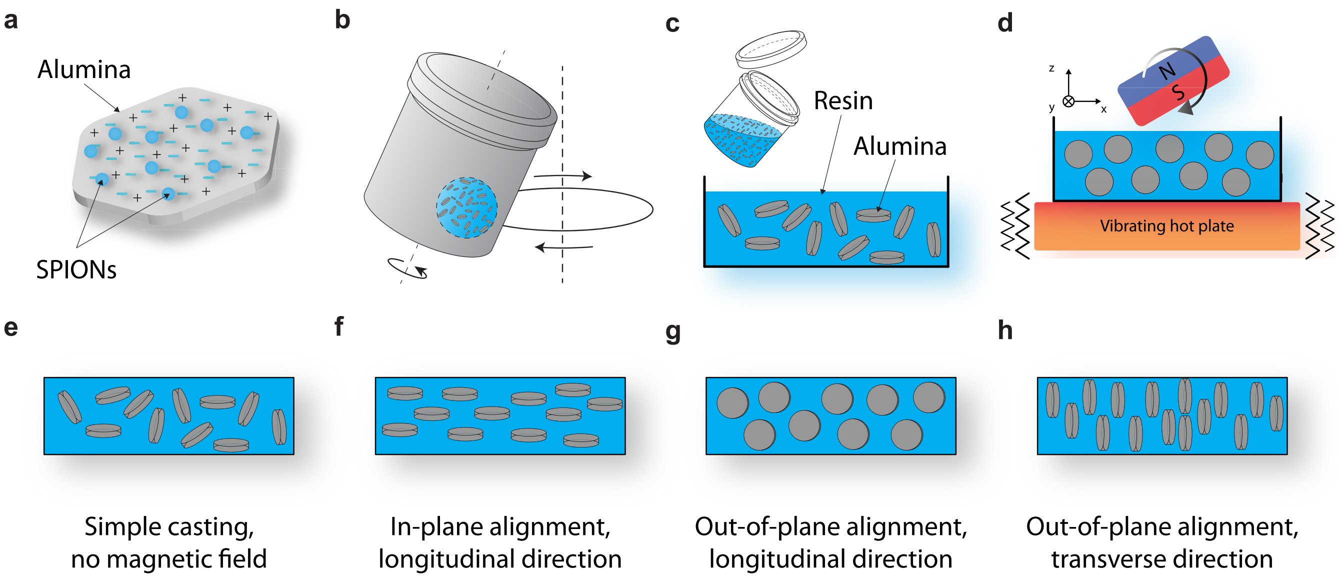

Figure 1. Manufacturing route and reinforcement architecture of the investigated platelet-reinforced polymers. (a) Alumina platelets electrostatically coated with superparamagnetic iron oxide nanoparticles (SPIONs). (b) Mixing and degassing of a suspension of coated platelets dispersed in a reactive liquid resin. (c) Casting of the suspension of platelets into a silicone mold. (d) Resin curing at 60 °C under an external rotating magnetic field assisted by a vibrating hot plate. (e−h) Final composites with four distinct reinforcement architectures comprising platelets with (e) alignment imposed by simple casting, (f) in-plane magnetic alignment in the longitudinal direction, (g) out-of-plane magnetic alignment in the longitudinal direction, and (h) out-of-plane magnetic alignment in the transverse direction.

Nature showcases many examples of composites that combine stiff and soft building blocks into rich reinforcement architectures over multiple length scales.[17−19] Highly mineralized biological composites, such as bone, tooth enamel, and mollusk shells, for example, exhibit particularly interesting reinforcement architectures consisting of staggered stiff elements surrounded by a continuous softer matrix. The high stiff−soft interfacial area and high volume fraction of the stiff phase achieved with this architectural motif allow the composite to attain antagonistic mechanical properties such as high stiffness and high fracture toughness.[20,21] In contrast to polymers with conventional fillers, recent studies suggest that the staggered architecture is also expected to increase the stiffness and the damping ability of the composite simultaneously.[22,23] This results from the strong reinforcing effect of the stiff elements combined with the highly dissipative response of the surrounding polymer phase when the composite is subjected to oscillatory loading conditions. In spite of the extensive research dedicated to the development of nacre-like materials with enhanced fracture strength and toughness,[24−26] the resulting bio-inspired composites have not been yet fully characterized in terms of damping behavior. Attempts to replicate the staggered design in synthetic systems led to 3D printed materials with improved damping properties.[23,27] However, the high mechanical compliance of the reinforcing elements used in these synthetic materials has limited significantly the absolute stiffness achieved.

Here, we manufacture and investigate the stiffness and damping response of platelet-reinforced polymers exhibiting a biologically inspired staggered reinforcement architecture. The staggered arrangement of platelets is generated by using either a simple casting or a magnetically assisted assembly process previously reported for the fabrication of highly aligned nacre-like composites.[11,28] Specimens with distinct reinforcement architectures are obtained by controlling the direction of the magnetic field applied during the process. The mechanical properties of such composites are then studied by performing dynamic mechanical analysis on specimens with different concentrations of alumina platelets in epoxy or poly(methyl methacrylate) matrices. The stiffness and damping properties of the obtained bio-inspired composites are rationalized by using an analytical micromechanical model and finally compared to the performance of other engineering and biological materials.

■ MATERIALS AND METHODS

The epoxy resin used as polymer matrix consisted of a diglycidyl ether of bisphenol A (Araldite LY 3585, Huntsman Advanced Materials, Switzerland). The resin was mixed with an amine hardener (Aradur 3475, Huntsman Advanced Materials, Switzerland) in a stoichiometric epoxy:hardener weight ratio of 100:21. The poly(methyl methacrylate) (PMMA) polymer matrix was produced by using a methyl methacrylate (MMA) (Elium 150, Arkema, France) cross-linked through radical polymerization with 3 vol % of the initiator and curing agent dibenzoyl peroxide (Perkadox CH-50X, provided by Arkema, France). Aluminum oxide (Al_2O_3) platelets (RonaFlair) with an aspect ratio in the range 17−26 were purchased from Merck, Germany. Polymers reinforced with platelets of this aspect ratio are expected to fail under the pull-out mode, thus enabling the onset of toughening mechanisms such as crack deflection and plastic deformation.[28,29] The platelets were surface functionalized with 12 nm superparamagnetic iron oxide nanoparticles (SPIONs) to become responsive in an external magnetic field.[28]

Specimens of platelet-reinforced polymers were fabricated by first suspending 10, 12.5, 17.5, 20, 25, and 30 vol % of functionalized platelets in uncured epoxy resin or MMA monomer by using a planetary mixer (ARE-250, Thinky, Japan). Samples without platelets were also produced and used as references. Platelets and resin were mixed and degassed for 5 and 8 min, respectively, at a rotational speed of 2000 rpm. Hardener (for epoxy) and initiator (for PMMA) were mixed into the suspensions for 1 min, and the resulting mixture was degassed again for another 5 min. Three-component suspensions were then casted into 30 mm × 80 mm silicone molds, which were placed on a hot plate heated to 60 °C. The external magnetic field and the temperature were kept constant for 1 and 3 h, respectively, to allow

https://dx.doi.org/10.1021/acsapm.0c00568
ACS Appl. Polym. Mater. 2020, 2, 3557−3565

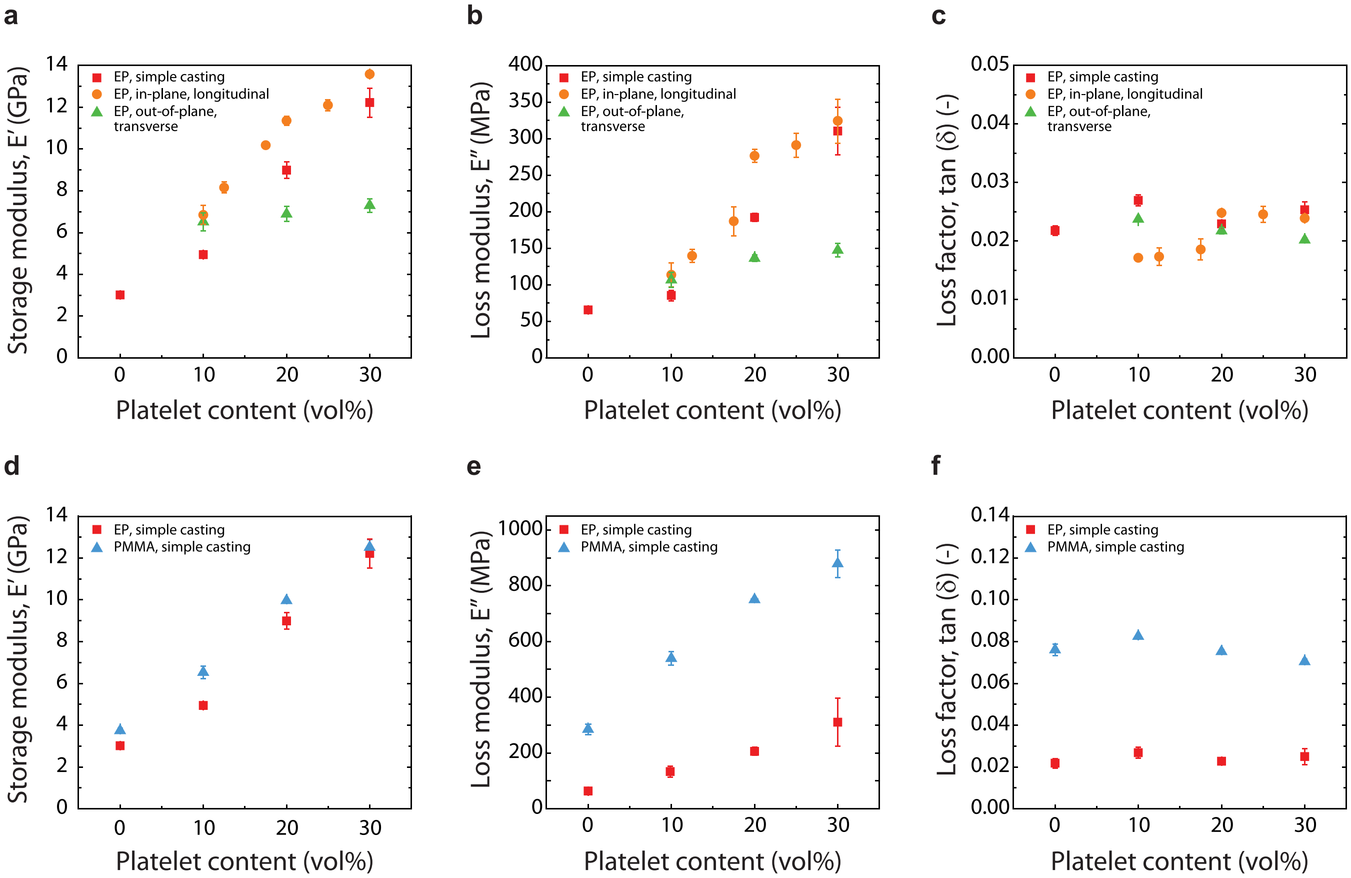

Figure 2. Mechanical properties under oscillatory deformation of composites with increasing platelet concentrations and distinct reinforcement architectures. (a, d) Storage modulus (E'), (b, e) loss modulus (E''), and (c, f) loss factor ($\tan(\delta)$) of composites prepared with (a−c) thermoset epoxy (EP) or (d−f) thermoplastic poly(methyl methacrylate) (PMMA) as polymer matrix. The effect of the reinforcement architecture is investigated for epoxy-based specimens with different platelet volume fractions. Composites with EP or PMMA as polymer matrix are compared by using cast specimens prepared in the absence of an external magnetic field.

for curing of the epoxy and PMMA phases. A magnetic field of 200 mT rotating at a frequency of 3 Hz was applied to enable biaxial alignment of the platelets. Postcuring was performed at 80 °C for 1 h.

Samples for mechanical testing were produced by grinding cast plates in a laboratory polishing machine (LapPol-25, Struers GmbH, Germany) and cutting them into precise bars by using a cutting machine equipped with a diamond cutoff wheel blade (Accutom-100, Struers GmbH, Germany). The feeding speed was set to 0.050 mm/s to guarantee damage-free surfaces. Prior to testing, the samples were stored for at least 24 h at 23 °C and 65% relative humidity. Nominal dimensions of the specimens were $2 \times 2 \times 30$ mm^3.

Dynamic mechanical analysis (DMA) was performed on a Q800 instrument (TA Instruments, USA) using a friction-reduced three-point bending setup with a 20 mm span. The specimens were preloaded with a flexural force of 0.1 N to conduct the measurement in the positive deflection regime. Frequency sweeps were performed between 1 and 100 Hz while keeping the displacement amplitude set to 40 μm. Amplitude sweeps were conducted with a displacement range of 5−100 μm at constant frequency of 10 Hz. A total number of eight measurements were considered for calculating the arithmetic average and standard deviation for each set of samples with a given reinforcement architecture and platelet volume fraction. The storage modulus, E', the loss modulus, E'', and the loss factor, tan (δ), were calculated from the measured complex modulus, E^*.

Microstructural images of polished and fractured samples were acquired by using a scanning electron microscope (Leo 1530 Gemini, Zeiss) operated with an acceleration voltage of 3 kV. Before imaging, the samples were coated with a 5 nm platinum layer using a compact coating unit (CCU-010, Safematic).

RESULTS AND DISCUSSION

Platelet-containing polymers with four distinct reinforced architectures were manufactured by using a simple magnetically assisted assembly process (Figure 1).[28,30] In this approach, platelets are first coated with superparamagnetic iron oxide nanoparticles (SPIONs) to enable orientation control under an external magnetic field. Next, the coated platelets are suspended in a reactive liquid resin and aligned in specific orientations by using an external magnet while the resin is cured with a hot plate. To achieve biaxial alignment of the platelets, the magnet is rotated at a certain fixed frequency above which the viscous forces exerted by the suspending liquid constrain the platelet motion to the plane of the rotating magnetic field.[30] This critical frequency depends on the aspect ratio of the platelets, the magnetization achieved with the SPION coating, the viscosity of the suspending medium, and the applied magnetic field. For the experimental system investigated here, the critical frequency is estimated to lie within the range 0.2−2.5 Hz. This critical frequency range was estimated by using a previously proposed model,[31] assuming an applied magnetic field of 0.2 T, a volume susceptibility of the platelet magnetic shell of 1.33, a platelet thickness of 370 nm, a platelet diameter of 8.3 μm, and a magnetic shell thickness of 12 nm. Because the viscosity of the epoxy resin is expected to drop from 40 to 4 Pa·s[32] during the beginning of

https://dx.doi.org/10.1021/acsapm.0c00568
ACS Appl. Polym. Mater. 2020, 2, 3557−3565

the thermal curing process, a lower and an upper bound were obtained for the critical frequency estimate.

Using this directed assembly technology, we created composite architectures with platelets aligned in-plane in the longitudinal direction and out-of-plane in the longitudinal or transverse direction. In another experimental series, specimens were also manufactured by simple casting in the absence of the external magnetic field. Composites with platelet concentrations in the range 5−30 vol % can be prepared by using this methodology. At the highest platelet content of 30 vol %, vibration of the casting mold was required to lower the viscosity of the suspension and thus ensure alignment under the external magnetic field.

The reinforcement architecture of the platelet-laden polymers affects directly the mechanical behavior of the composites when subjected to oscillatory mechanical loading (Figure 2). The mechanical response of the composite to oscillatory deformations was quantified in terms of the storage modulus (E'), loss modulus (E''), and the loss factor ($\tan(\delta)$). Preliminary dynamic mechanical analysis (DMA) showed that all investigated materials exhibit linear viscoelastic properties if probed at a constant displacement amplitude of 40 μm in the frequency range 1−100 Hz (see the Supporting Information, section SI 1). To systematically evaluate the effect of the reinforcement architecture on the mechanical properties of the composite, we compare the E', E'', and $\tan(\delta)$ values obtained at the exemplary frequency of 10 Hz.

DMA data measured for specimens prepared with an epoxy matrix indicate that the addition of 30 vol % alumina platelets increases the storage and loss moduli of the polymer by a factor of 4.5 and 5, respectively (Figure 2a,b). The observed reinforcing effect is most pronounced when the platelets are magnetically aligned in the longitudinal direction parallel to the oscillatory stresses that develop within the material. This is evidenced by the up to 90% higher E' values measured for composites featuring in-plane platelets with longitudinal orientation compared to specimens containing platelets aligned in the out-of-plane transverse direction. Interestingly, platelets oriented in the longitudinal direction show a similar reinforcing effect no matter if the alignment occurs within the plane or in an out-of-plane configuration (see the Supporting Information, section SI 2).

A similar trend is observed for the loss moduli (E'') of composites exhibiting in-plane and out-of-plane platelet orientation. Samples made by simple casting in the absence of a magnetic field showed intermediate reinforcement levels for platelet concentrations in the range between 20 and 30 vol %. The weaker mechanical properties of specimens with lower particle contents are presumably caused by the higher rotational freedom of the platelets under this more diluted condition. Such rotational freedom is reduced when the volume fraction exceeds the critical concentration at which the platelets are expected to assemble into colloidal liquid crystalline domains. For the platelets with aspect ratio of 17−26 used in this work, this critical volume fraction lies between 21 and 32 vol %.[33] Our results therefore suggest that the strong reinforcement effect achieved in cast samples containing 20 and 30 vol % platelets might arise from the formation of liquid crystalline domains that partially orient within the plane during casting of the composite resin.

Importantly, the observed increase in E' and E'' for high platelet concentrations is achieved without compromising the energy dissipation properties of the polymer matrix. Indeed, the loss factor $\tan(\delta)$ was found to vary only slightly with the volume fraction of platelets and to be less sensitive to the platelet orientation (Figure 2c). Because the loss factor of the composite is determined by the properties of the polymer matrix, samples with poly(methyl methacrylate) (PMMA) as a polymer phase that is inherently more dissipative were also prepared and mechanically tested (Figure 2d−f). For these PMMA-based composites, no magnetic field was applied during curing. Following the results obtained with the epoxy matrix, the absence of a magnet in the experimental setup is expected to facilitate the processing of the composite while still reaching a high degree of platelet alignment. This is especially valid at high volume fractions of particles, where magnetically assisted particle alignment is found to be more challenging. Indeed, electron microscopy and image analysis of PMMA-based composites with 30 vol % platelets confirm that the simple casting procedure is sufficient to achieve a level of alignment comparable to that obtained in previous work in other bio-inspired composites containing a similar volume fraction of magnetically oriented platelets (see the Supporting Information, section SI 3).[11]

Results of the dynamic mechanical analysis reveal that the PMMA-based composites reach the same level of mechanical reinforcement (E), while enhancing significantly the loss modulus (E'') and the loss factor ($\tan(\delta)$) of the material. Such enhancement is most pronounced for specimens containing the highest platelet volume fraction of 30 vol %, which reached E'' and $\tan(\delta)$ values that increased by a factor of respectively 2.7 and 2.9 compared to the level observed for composites prepared with the less dissipative epoxy matrix. The high dissipative properties of the PMMA matrix arise from the enhanced motion of the ester side groups of this polymer at room temperature. The motion of such side groups is facilitated by the large free volume of this polymer and is usually known as a β relaxation process. Such a dissipative process occurs at temperatures much lower than the glass transition temperature associated with α relaxation (130−140 °C).[34]

The effect of the volume fraction of platelets on the dynamic mechanical properties of the composites can be rationalized on the basis of micromechanical models developed for soft materials reinforced with discontinuous stiff elements.[27] By use of a tension-shear chain (TSC) model, the storage and loss moduli of composites with nacre- and bone-like staggered architecture were shown to depend on the volume fraction of platelets (ϕ) as follows:

$$\frac{1}{E'} = \frac{1}{E'_{\mathrm{p}}\varphi} + \frac{4(1-\varphi)}{\alpha G'_{\mathrm{m}}\varphi^2\rho^2} \tag{1}$$

and

$$E'' = \frac{4E'_{\mathrm{p}}2\rho^2(1-\varphi)\alpha G''_{\mathrm{m}}}{[\alpha G'_{\mathrm{m}}\rho^2 + 4E'_{\mathrm{p}}(\varphi^{-1}-1)]^2} \tag{2}$$

where E'_{p} is the storage modulus of the stiff platelet; G'_{m} and G''_{m} are the storage and loss shear moduli of the softer continuous matrix, respectively; ρ is the aspect ratio of the platelet; and α is a parameter that quantifies the ability of the continuous matrix to carry tensile load at the end of adjacent platelets (see the Supporting Information, section SI 4). The loss factor ($\tan(\delta)$) can be directly obtained from these equations via the relation $\tan(\delta) = E''/E'$.

https://dx.doi.org/10.1021/acsapm.0c00568
ACS Appl. Polym. Mater. 2020, 2, 3557−3565

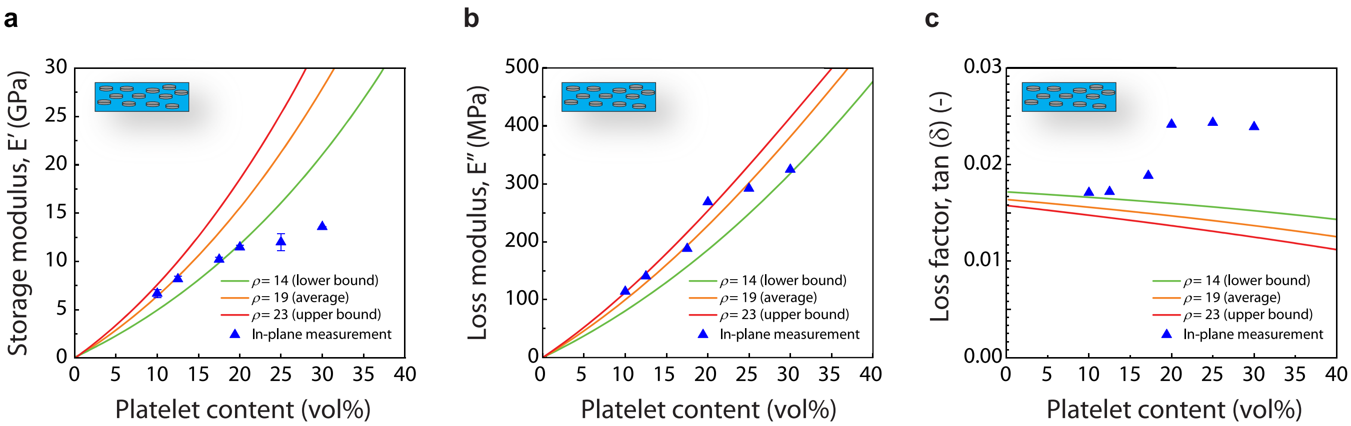

Figure 3. Dynamic mechanical properties of platelet-reinforced polymers compared to theoretical predictions for composites with longitudinal staggered architecture. (a−c) Effect of the volume fraction of alumina platelets on the (a) storage modulus (E'), (b) loss modulus (E''), and (c) loss factor ($\tan(\delta)$) of in-plane reinforced composites containing a thermoset epoxy as polymer matrix. Full lines show the theoretical prediction for epoxy reinforced with alumina platelets featuring aspect ratios corresponding to the average values as well as the upper and lower bounds of the experimental particle size distribution.

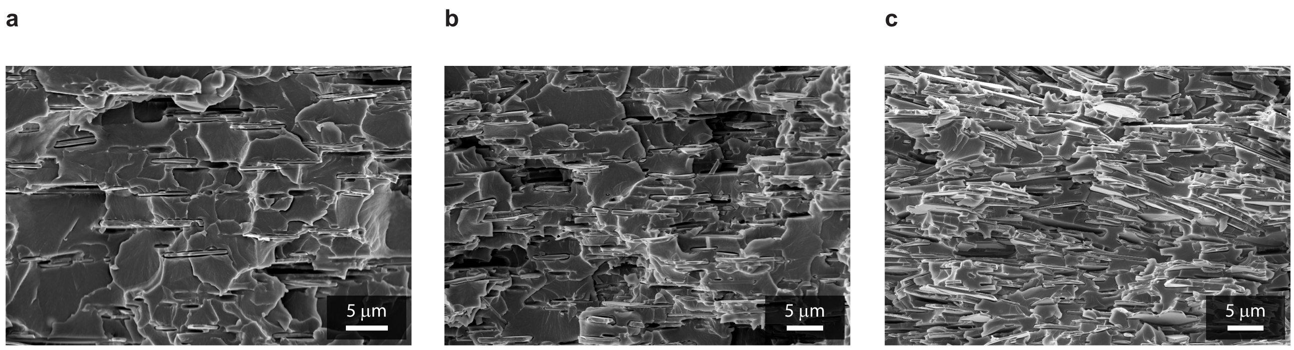

Figure 4. Scanning electron micrographs of epoxy samples reinforced with (a) 10, (b) 20, and (c) 30 vol % of alumina platelets with in-plane alignment in the longitudinal direction.

To test the validity of the staggered composite model for our platelet-reinforced polymers, we compare the obtained experimental data with theoretical predictions of E', E'', and $\tan(\delta)$ based on the equations above (Figure 3). Because the alumina platelets utilized in this work display polydisperse sizes and aspect ratios, model predictions are shown for aspect ratios corresponding to the upper and lower bounds of the measured size distributions (see the Supporting Information, section SI 5). Upper and lower bounds were defined as the aspect ratio corresponding to $\overline{\mu} + \Delta$ and $\overline{\mu} - \Delta$, respectively, where $\overline{\mu}$ is the mean platelet size and Δ is the standard deviation of the Gaussian distribution.

The comparison between experimental data and analytical predictions indicates that the loss modulus of the epoxy-based composites falls predominantly within the upper and lower bounds given by the staggered model (Figure 3b). In terms of storage modulus, an agreement between theory and experiments is observed for composites containing platelet volume fractions below 17.5 vol % (Figure 3a). Specimens with platelets above this concentration exhibit storage modulus lower than the prediction values, most probably due to the poorer alignment of alumina platelets at this high particle content. Indeed, the high viscosity of epoxy resins with 30 vol % alumina is expected to hinder the magnetic alignment of the platelets under the magnetic fields generated in our experimental setup. Electron microscopy imaging confirms the slight platelet misalignment of such composites in comparison to specimens containing lower platelet content (Figure 4). Because the loss factor is inversely proportional to the storage modulus ($\tan(\delta) = E''/E'$), the lower E' values of composites with more than 17.5 vol % platelets eventually increases the $\tan(\delta)$ level reached by samples loaded with high particle concentrations. As a result, the experimentally measured loss factor of composites with 20−30 vol % platelets are 59−104% higher compared to the theoretical predictions (Figure 3c). The ability to describe the experimentally measured E'' demonstrates that the assumptions underlying the tension-shear chain model are valid for this specific mechanical property but do not necessarily apply for E' and $\tan(\delta)$ of the composite. This analysis suggests that the slight platelet misalignment observed at higher particle concentrations is more detrimental to the storage modulus than to the loss modulus of the composite. Further studies are needed to elucidate the underlying reasons for the observed discrepancies between theory and experiments.

The good agreement between the theoretical predictions and the experimentally measured E'' data has important practical implications, since the loss modulus is often taken as the relevant figure of merit for damping applications. Indeed, materials with high loss modulus combine high stiffness and enhanced energy dissipation.[27] To establish guidelines for the design of biologically inspired composites combining these two properties, we created a design map that displays the loss modulus of composites containing alumina platelets in an

https://dx.doi.org/10.1021/acsapm.0c00568
ACS Appl. Polym. Mater. 2020, 2, 3557−3565

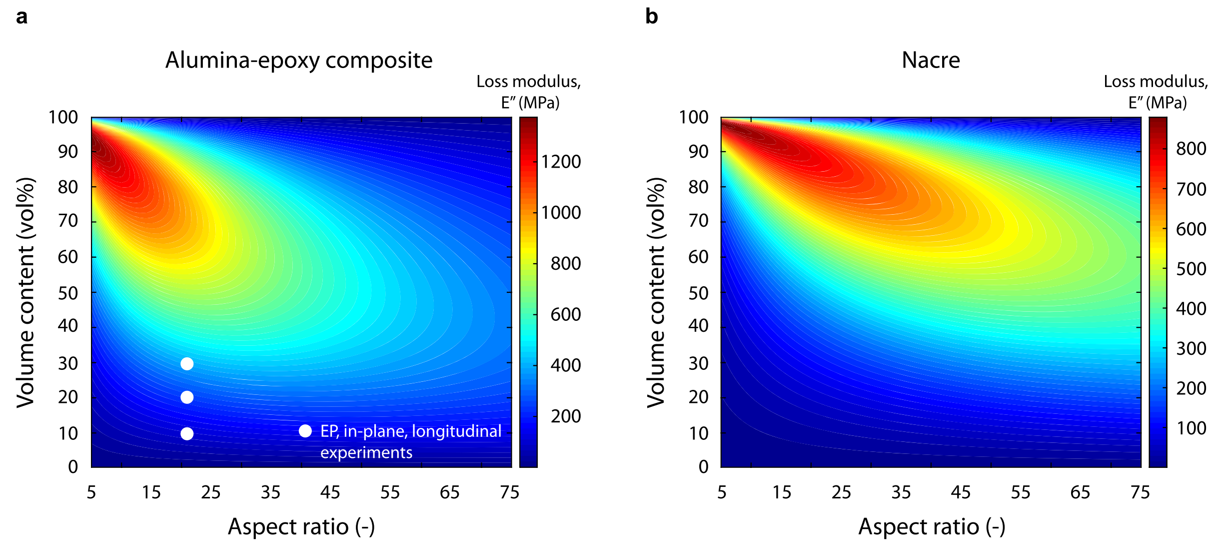

Figure 5. Design maps indicating the range of platelet volume fractions and aspect ratios leading to staggered composites with maximum loss modulus. The contour lines show theoretical predictions of the loss modulus for (a) alumina platelets ($E_p' = 300$ GPa) in an epoxy matrix ($G_m' = 1.16$ GPa and $G_m'' = 0.023$ GPa) and (b) aragonite platelets ($E_p' = 70$ GPa)[35] in a biopolymer matrix ($G_m' = E_p'/1000 = 0.07$ GPa and $G_m'' = 0.003589$ GPa).[19,27] The shear loss modulus of the nacreous biopolymer matrix, G_m'', was estimated from dynamical mechanical analysis measurements on nacre samples (see the Supporting Information, section SI 6). The white symbols shown in (a) represent the volume fractions of platelets (of fixed aspect ratio) utilized in the composites investigated in this work.

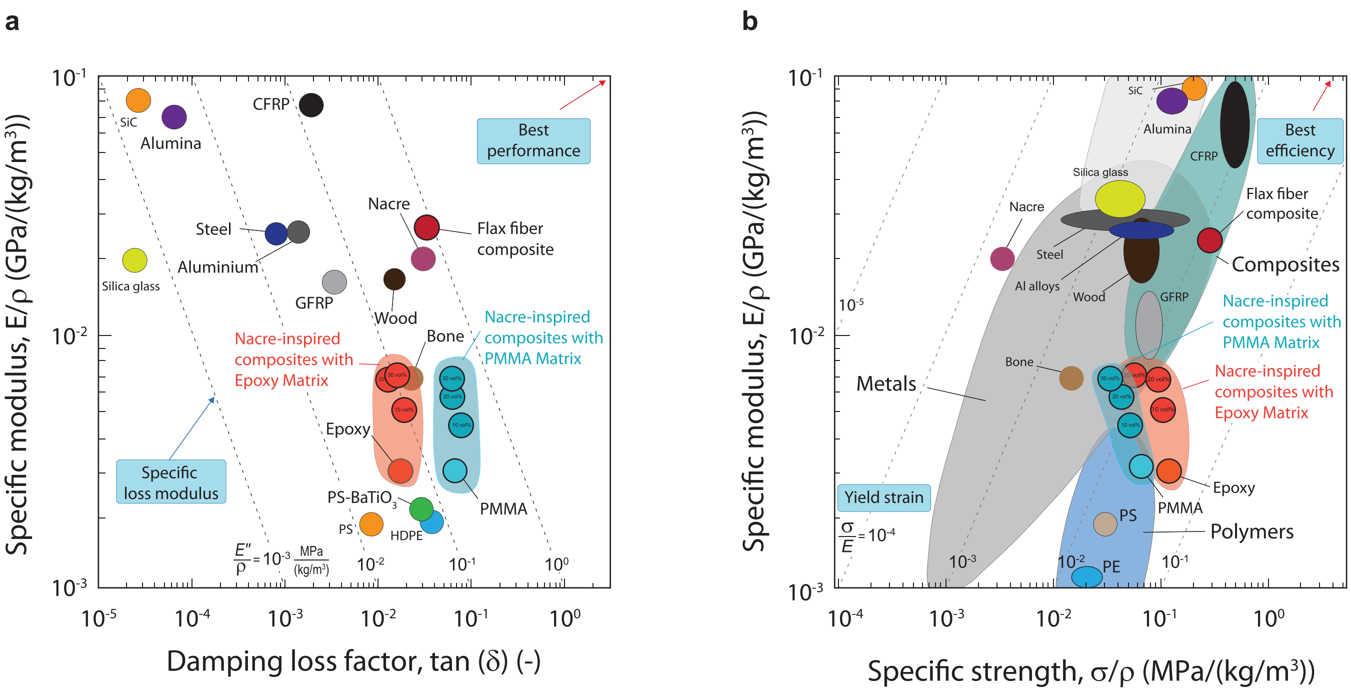

Figure 6. Ashby diagrams displaying the mechanical properties of the bio-inspired platelet-reinforced composites in comparison to those of other engineering and biological materials. The specific modulus (E/ρ) is plotted against the (a) loss factor ($\tan(\delta)$) or (b) the specific strength (σ/ρ) for a broad range of structural materials. Data were obtained from Lakes,[37] CES EduPack,[38] and Unwin et al. ($PS\text{-}BaTiO_3$).[16]

epoxy matrix based on the TSC model (Figure 5a). Such a map is compared to a contour plot that predicts the loss modulus of nacre by using the same staggered composite model (Figure 5b). The materials' properties of the nacre constituents were estimated from actual measurements on nacre samples (see the Supporting Information, section SI 6). Although the presence of mineral bridges and nanoasperities are not explicitly considered in the staggered model, we expect these important structural features to be taken into account by estimating the effective shear properties of the biopolymer matrix from actual measured data. In the final contour plot, the volume fraction (φ) and the aspect ratio (ρ) of platelets were selected as main design parameters for the optimization of the loss modulus of the composites.

For both design maps, the maximum loss modulus is observed at specific platelet concentrations (φ_{opt}) and aspect ratios (ρ_{opt}). This reflects the two different regimes that control the damping behavior of the composites.[23] For $\varphi < \varphi_{opt}$ and $\rho < \rho_{opt}$, the damping response of the composites is dictated by the polymer phase, and the loss modulus is found to increase

https://dx.doi.org/10.1021/acsapm.0c00568
ACS Appl. Polym. Mater. 2020, 2, 3557−3565

with the particle volume fraction and aspect ratio. In this regime, energy dissipation occurs primarily through shearing of the viscoelastic polymer matrix in between the stiff oriented platelets. By contrast, composites with $\varphi > \varphi_{opt}$ and $\rho > \rho_{opt}$ exhibit damping properties dominated by the stiff and hard platelets. Under this condition, the loss modulus decreases with the volume fraction and the aspect ratio of the particles, since energy dissipation within the polymer matrix is suppressed by the stiffening effect of the stiff platelets.

The design maps also reveal that the ρ values that maximize the loss modulus (ρ_{opt}) are significantly different for the alumina-reinforced epoxy compared to biological nacre. Such difference arises primarily from the fact that the alumina platelets display a storage modulus (E'_p) that is about 4 times of the carbonate platelets present in nacre. Because of the stiffer platelets, the E'' value of the alumina-reinforced polymer shows a maximum at significantly lower aspect ratios (ρ_{opt}) compared to the biological material. This analysis highlights the importance of mimicking the quantitative design principle (staggered composite model) and not the structure of the biological material per se when applying bio-inspired concepts for the creation of enhanced engineering materials. Indeed, a hypothetical composite containing alumina platelets and epoxy with φ and ρ values that are optimum for nacre would exhibit loss modulus that is less than 20% of the maximum level theoretically achievable by synthetic composites reinforced with such stiff particles.

Importantly, the use of stiff alumina platelets leads to an optimum aspect ratio (ρ_{opt}) that is still relatively close to the ρ values of commercially available platelets that can be easily processed through the magnetic assembly technology utilized in this study. This allows us to leverage the potential of the stiff alumina platelets for its ability to simultaneously reinforce the polymer matrix and promote strong shear-induced energy dissipation within the polymer. Although the optimum volume fraction of platelets (φ_{opt}) is not experimentally accessible with the utilized fabrication process, the design map shows that increasing the concentration of platelets is an effective strategy to enhance the loss modulus of this platelet−polymer system (Figure 5a).

When plotted in an Ashby diagram, our experimental data clearly reveal the beneficial effect of the staggered architecture (Figure 6a). By increasing the storage modulus of the composite (E') without compromising its ability to dissipate energy ($\tan(\delta)$), the addition of staggered platelets to an epoxy matrix enhances its loss modulus to levels comparable to those of bone. The replacement of the epoxy matrix by poly(methyl methacrylate) (PMMA) improves the loss modulus further, resulting in composites with damping characteristics that are superior to bone and on par with nacre. In fact, our stiffest PMMA-based bio-inspired material shows a loss modulus comparable to that of flax fiber-reinforced polymers, which are known for their very high damping performance.[4,36] The difference between composites reinforced with flax fibers and alumina platelets lies in the storage modulus and the loss factor. Whereas polymers containing flax fibers reach high loss modulus through an increase in storage modulus, the platelet-reinforced composites do so by enhancing the material's loss factor. Despite their lower stiffness, the incorporation of staggered platelets into PMMA and epoxy leads to composites with mechanical properties approaching the specific storage modulus and specific mechanical strength of metals and glass fiber-reinforced polymers (GFRP, Figure 6b). Compared to 3D printed polymers with staggered architecture,[23] the bio-inspired composites reported here showcase damping performance (E'') that is 50% higher while improving the stiffness (E') by a factor of 26. This results from the much smaller length scales, higher platelet−matrix interfacial area, and enhanced stiffness of the alumina platelets used in the bio-inspired composites in comparison to the 3D printed all-polymer counterparts. The damping performance of our staggered composites is also superior to the exceptionally high values recently achieved by using stiff polymers loaded with polyurethane-coated inorganic fillers.[16] In this case, the platelet-reinforced architecture reported not only enhances the damping performance but also increases by a factor of 5 the fracture toughness of the composite.[11]

CONCLUSIONS

The reinforcement of polymers by using stiff alumina platelets arranged in a bio-inspired staggered architecture increases the stiffness of the polymer by a factor of up to 4.5 without compromising its high damping characteristics. Strong platelet alignment can be achieved either by simple casting of suspensions with high particle content or by using an external magnetic field. A simple micromechanical model for staggered architectures captures reasonably well the mechanical properties of such bio-inspired composites under oscillatory bending conditions. Such a model allows one to predict the volume fraction and aspect ratio of platelets that maximizes the damping performance of the composite. Importantly, the optimum aspect ratio for the synthetic alumina platelets is about half that of the aragonite tablets found in the nacreous layer of mollusk shells. Therefore, the nacre-inspired composites developed in this study well illustrates the importance of replicating the structural design principle of the biological material rather than the microstructure per se. Following this approach, synthetic composites with damping performance superior to bone and comparable to nacre could be produced by using much lower volume fractions of reinforcing platelets. These experimental findings should aid the design and manufacturing of future structural materials combining mechanical stiffness with low-energy passive damping behavior.

ASSOCIATED CONTENT

Supporting Information

The Supporting Information is available free of charge at https://pubs.acs.org/doi/10.1021/acsapm.0c00568.

Effect of frequency on the dynamic mechanical properties of the composites; viscoelastic properties of composites containing platelets aligned longitudinally in-plane or out-of-plane; platelet orientation in PMMA-based composite; tension-shear chain model; size distribution of the alumina platelets; determination of the shear loss modulus of the nacre matrix (PDF)

AUTHOR INFORMATION

Corresponding Authors

Kunal Masania − *Complex Materials, Department of Materials, ETH Zürich, 8093 Zürich, Switzerland;* orcid.org/0000-0001-9498-1505; Email: k.masania@tudelft.nl

André R. Studart − *Complex Materials, Department of Materials, ETH Zürich, 8093 Zürich, Switzerland;*

orcid.org/0000-0003-4205-8545; Email: andre.studart@mat.ethz.ch

Authors

Wilhelm Woigk − *Complex Materials, Department of Materials, ETH Zürich, 8093 Zürich, Switzerland*

Fabian Stork − *Complex Materials, Department of Materials, ETH Zürich, 8093 Zürich, Switzerland*

Alex Heusi − *Complex Materials, Department of Materials, ETH Zürich, 8093 Zürich, Switzerland*

Erik Poloni − *Complex Materials, Department of Materials, ETH Zürich, 8093 Zürich, Switzerland*

Complete contact information is available at: https://pubs.acs.org/10.1021/acsapm.0c00568

Notes

The authors declare no competing financial interest.

■ ACKNOWLEDGMENTS

We thank the Gebert Rüf Stiftung (Grant GRS-077/15), the Innosuisse funding programme (Grant 18848.1), and the Swiss Competence Center for Energy Research (Capacity Area A3: Minimization of energy demand) for the financial support. The research also benefitted from support from the Swiss National Science Foundation within the framework of the National Center of Competence in Research for Bio-Inspired Materials. We also thank Dr. Dimitri Kokkinis for the microscopy images of the platelets, Prof. Dr. Erich Kramer for helpful discussions, and the Institute of Polymer Engineering at the FHNW University of Applied Sciences and Arts Northwestern Switzerland for kindly providing access to analytical equipment.

■ REFERENCES

(1) Seong, M. S.; Choi, S. B.; Kim, C. H. Damping force control of frictionless MR damper associated with hysteresis modeling. *J. Phys.: Conf. Ser.* **2013**, *412*, 012044.

(2) Rao, M. D. Recent applications of viscoelastic damping for noise control in automobiles and commercial airplanes. *J. Sound Vib* **2003**, *262*, 457−74.

(3) Taniguchi, M.; Fujita, K.; Tsuji, M.; Takewaki, I. Hybrid control system for greater resilience using multiple isolation and building connection. *Front Built Environ* **2016**, *2*, 1−10.

(4) Rueppel, M.; Rion, J.; Dransfeld, C.; Fischer, C.; Masania, K. Damping of carbon fibre and flax fibre angle-ply composite laminates. *Compos. Sci. Technol.* **2017**, *146*, 1−9.

(5) Duc, F.; Bourban, P. E.; Månson, J. A. E. The role of twist and crimp on the vibration behaviour of flax fibre composites. *Compos. Sci. Technol.* **2014**, *102*, 94−9.

(6) Maheri, M. R.; Adams, R. D. NII-Electronic Library Service. *JSME Int. J., Ser. A* **1999**, *42*, 307−20.

(7) Chandra, R.; Singh, S. P.; Gupta, K. A study of damping in fiber-reinforced composites. *J. Sound Vib* **2003**, *262*, 475−96.

(8) Zhou, X. Q.; Yu, D. Y.; Shao, X. Y.; Zhang, S. Q.; Wang, S. Research and applications of viscoelastic vibration damping materials: A review. *Compos Struct* **2016**, *136*, 460−80.

(9) Sun, L.; Gibson, R. F.; Gordaninejad, F.; Suhr, J. Energy absorption capability of nanocomposites: A review. *Compos. Sci. Technol.* **2009**, *69*, 2392−409.

(10) Wei, W.; Zhang, Y.; Liu, M.; Zhang, Y.; Yin, Y.; Gutowski, W. S.; Deng, P.; Zheng, C. Improving the damping properties of nanocomposites by monodispersed hybrid POSS nanoparticles: Preparation and mechanisms. *Polymers (Basel, Switz.)* **2019**, *11*, 1−15.

(11) Libanori, R.; Erb, R. M.; Studart, A. Mechanics of Platelet-Reinforced Composites Assembled Using Mechanical and Magnetic Stimuli. *ACS Appl. Mater. Interfaces* **2013**, *5*, 10794−10805.

(12) Shukla, D. K.; Kasisomayajula, S. V.; Parameswaran, V. Epoxy composites using functionalized alumina platelets as reinforcements. *Compos. Sci. Technol.* **2008**, *68*, 3055−63.

(13) Oner Ekiz, O.; Dericioglu, A. F.; Kakisawa, H. An efficient hybrid conventional method to fabricate nacre-like bulk nano-laminar composites. *Mater. Sci. Eng., C* **2009**, *29*, 2050−4.

(14) Gurbuz, S. N.; Dericioglu, A. F. Effect of reinforcement surface functionalization on the mechanical properties of nacre-like bulk lamellar composites processed by a hybrid conventional method. *Mater. Sci. Eng., C* **2013**, *33*, 2011−9.

(15) Libanori, R.; Münch, F. H. L.; Montenegro, D. M.; Studart, A. R. Hierarchical reinforcement of polyurethane-based composites with inorganic micro- and nanoplatelets. *Compos. Sci. Technol.* **2012**, *72*, 435−45.

(16) Unwin, A. P.; Hine, P. J.; Ward, I. M.; Fujita, M.; Tanaka, E.; Gusev, A. A. Escaping the Ashby limit for mechanical damping/stiffness trade-off using a constrained high internal friction interfacial layer. *Sci. Rep.* **2018**, *8*, 1−10.

(17) Fratzl, P.; Weinkamer, R. Nature's hierarchical materials. *Prog. Mater. Sci.* **2007**, *52*, 1263−334.

(18) Wegst, U. G. K.; Bai, H.; Saiz, E.; Tomsia, A. P.; Ritchie, R. O. Bioinspired structural materials. *Nat. Mater.* **2015**, *14*, 23−36.

(19) Ji, B.; Gao, H. Mechanical properties of nanostructure of biological materials. *J. Mech. Phys. Solids* **2004**, *52*, 1963−90.

(20) Gao, H. Application of fracture mechanics concepts to hierarchical biomechanics of bone and bone-like materials. *Int. J. Fract.* **2006**, *138*, 101−37.

(21) Barthelat, F.; Dastjerdi, A. K.; Rabiei, R. An improved failure criterion for biological and engineered staggered composites. *J. R. Soc., Interface* **2013**, *10*, 20120849−20120849.

(22) Qwamizadeh, M.; Liu, P.; Zhang, Z.; Zhou, K.; Wei Zhang, Y. Hierarchical Structure Enhances and Tunes the Damping Behavior of Load-Bearing Biological Materials. *J. Appl. Mech.* **2016**, *83*, 051009.

(23) Zhang, P.; Heyne, M. A.; To, A. C. Biomimetic staggered composites with highly enhanced energy dissipation: Modeling, 3D printing, and testing. *J. Mech. Phys. Solids* **2015**, *83*, 285−300.

(24) Grossman, M.; Bouville, F.; Erni, F.; Masania, K.; Libanori, R.; Studart, A. R. Mineral Nano-Interconnectivity Stiffens and Toughens Nacre-like Composite Materials. *Adv. Mater.* **2017**, *29*, 1605039.

(25) Grossman, M.; Pivovarov, D.; Bouville, F.; Dransfeld, C.; Masania, K.; Studart, A. R. Hierarchical Toughening of Nacre-Like Composites. *Adv. Funct. Mater.* **2019**, *29*, 1806800.

(26) Magrini, T.; Bouville, F.; Lauria, A.; Le Ferrand, H.; Niebel, T. P.; Studart, A. R. Transparent and tough bulk composites inspired by nacre. *Nat. Commun.* **2019**, *10*, 1−10.

(27) Zhang, P.; To, A. C. Highly Enhanced Damping Figure of Merit in Biomimetic Hierarchical Staggered Composites. *J. Appl. Mech.* **2014**, *81*, 051015.

(28) Erb, R. M.; Libanori, R.; Rothfuchs, N.; Studart, A. R. Composites Reinforced in Three Dimensions by Using Low Magnetic Fields. *Science (Washington, DC, U. S.)* **2012**, *335*, 199−205.

(29) Bonderer, L. J.; Studart, A. R.; Gauckler, L. J. Bioinspired Design and Assembly of Platelet Reinforced Polymer Films. *Science (Washington, DC, U. S.)* **2008**, *319*, 1069−1073.

(30) Erb, R. M.; Segmehl, J.; Charilaou, M.; Löffler, J. F.; Studart, A. R. Non-linear alignment dynamics in suspensions of platelets under rotating magnetic fields. *Soft Matter* **2012**, *8*, 7604−9.

(31) Erb, R. M.; Segmehl, J.; Schaffner, M.; Studart, A. R. Temporal response of magnetically labeled platelets under dynamic magnetic fields. *Soft Matter* **2013**, *9*, 498−505.

(32) Geissberger, R.; Maldonado, J.; Bahamonde, N.; Keller, A.; Dransfeld, C.; Masania, K. Rheological modelling of thermoset composite processing. *Composites, Part B* **2017**, *124*, 182−9.

(33) Le Ferrand, H.; Bouville, F.; Studart, A. R. Design of textured multi-layered structures: Via magnetically assisted slip casting. *Soft Matter* **2019**, *15*, 3886−96.

(34) Schwarzl, F. R. *Polymermechanik: Struktur und mechanisches Verhalten von Polymeren*; Springer: Berlin, 1990.
(35) Jackson, A. P.; Vincent, J. F. V.; Turner, R. M. The mechanical design of nacre. *Proc. R Soc. London, Ser. B: Biol. Sci.* **1988**, *234*, 415−40.
(36) Duc, F.; Bourban, P. E.; Plummer, C. J. G.; Månson, J. -a. E. Damping of thermoset and thermoplastic flax fibre composites. *Composites, Part A* **2014**, *64*, 115−23.
(37) Lakes, R. S. High damping composite materials: Effect of structural hierarchy. *J. Compos. Mater.* **2002**, *36*, 287−297.
(38) *CES EduPack*; Granta Design Limited: Cambridge, UK, 2017.

https://dx.doi.org/10.1021/acsapm.0c00568
ACS Appl. Polym. Mater. 2020, 2, 3557−3565